

High light intensities can be used to grow healthy and robust cannabis plants during the vegetative stage of indoor production

Melissa Moher¹, David Llewellyn¹, Max Jones² and Youbin Zheng^{1,*}

¹School of Environmental Sciences and ²Department of Plant Agriculture, University of Guelph, 50 Stone Road East, Guelph, ON, N1G 2W1, Canada

*Corresponding author. E-mail address: yzheng@uoguelph.ca

Acknowledgement

We thank Ontario Centres of Excellence and HEXO Corp. for financial support and HEXO Corp. for providing the plant material and production space for this experiment. We also thank Bluelab Corporation for their measurement tools and to Scott Golem, Elizabeth Foley, Steve Dinka, and Allison Slater for their outstanding technical support during the trial.

Additional index words. Light-emitting diodes, PPFD, DLI, growth, morphology

Abstract.

Although the vegetative stage of indoor cannabis production can be relatively short in duration, there is a high energy demand due to higher light intensities (LI) than the clonal propagation stage and longer photoperiods than the flowering stage (i.e., 16 – 24 hours vs. 12 hours). While electric lighting is a major component of both energy consumption and overall production costs, there is a lack of scientific information to guide cultivators in selecting a LI that corresponds to their vegetative stage production strategies. To determine the vegetative plant responses to LI, clonal plants of ‘Gelato’ were grown for 21 days with canopy-level photosynthetic photon flux densities (PPFD) ranging between 135 and 1430 $\mu\text{mol}\cdot\text{m}^{-2}\cdot\text{s}^{-1}$ on a 16-hour photoperiod (i.e., daily light integrals of ≈ 8 to 80 $\text{mol}\cdot\text{m}^{-2}\cdot\text{d}^{-1}$). Plant height and growth index responded quadratically; the number of nodes, stem thickness, and aboveground dry weight increased asymptotically; and internode length and water content of aboveground tissues decreased linearly with increasing LI. Foliar attributes had varying responses to LI. Chlorophyll content index increased asymptotically, leaf size decreased linearly and specific leaf weight increased linearly with increasing LI. Generally, PPFD levels of $\approx 900 \mu\text{mol}\cdot\text{m}^{-2}\cdot\text{s}^{-1}$ produced compact, robust plants that are commercially relevant, while PPFD levels of $\approx 600 \mu\text{mol}\cdot\text{m}^{-2}\cdot\text{s}^{-1}$ promoted plant morphology with more open architecture – to increase airflow and reduce the potential foliar pests in compact (i.e., indica-dominant) genotypes.

Introduction

Drug-type cannabis is a high-value crop that is mainly grown in controlled environments [e.g., indoors (i.e., with no natural lighting) and greenhouses] where growing conditions can be maintained for consistent, year-round production (Benke and Tomkins, 2017; Despommier, 2013). Electricity costs are particularly high in indoor environments (Mills, 2012) because the

47 plants completely rely on electric light sources for providing photosynthetically active radiation
48 (*PAR*, 400-700 nm). Electric lighting is also used in greenhouse environments to provide
49 supplemental *PAR* when the natural light levels are insufficient [e.g., when daylengths are short
50 or when it is cloudy outside (Bilodeau et al., 2019)]. Since light has a major role in moderating
51 plant morphology and ontogeny, light intensity (LI), spectrum, and photoperiod can be
52 manipulated by the cultivator to produce plants with the desired morphological characteristics
53 during the various growth stages of indoor cannabis production; ultimately resulting in high yield
54 and quality of the marketable products (e.g., mature female inflorescences). Lighting-related
55 electricity consumption is also a major consideration, due to its exceptionally high cost (e.g., per
56 unit of crop yield) in indoor cannabis production (Arnold, 2013; Mehboob et al., 2020).

57
58 Each of three distinct growth stages that are commonly used in indoor cannabis production (i.e.,
59 propagation, vegetative growth, and flowering) have different photoperiod and LI requirements.
60 In the propagation stage, the photoperiod is generally 18 – 24 h (Chandra et al., 2020) and
61 canopy-level photosynthetic photon flux density (PPFD, $\mu\text{mol}\cdot\text{m}^{-2}\cdot\text{s}^{-1}$) is usually low (Fluence,
62 2020; Lumigrow, 2017) to minimize transpiration loss as the clonal plants establish new root
63 systems. After approximately two weeks in propagation, rooted cuttings (i.e., transplants)
64 transition into the vegetative stage (Caplan et al. 2018) where they are exposed to similar
65 photoperiods but higher PPFD than propagation to encourage strong vegetative growth to
66 prepare the plants for the flowering stage (Rodriguez-Morrison et al, 2021). After approximately
67 two to four weeks in the vegetative stage, plants are transitioned to a 12-h photoperiod and even
68 higher PPFD to enhance growth and yield. Depending on the genotype, indoor-grown cannabis
69 crops normally spend between 6 and 12 weeks under the 12-h flowering photoperiod before the
70 female inflorescences have reached optimum maturity for harvesting (Carpentier et al., 2012).

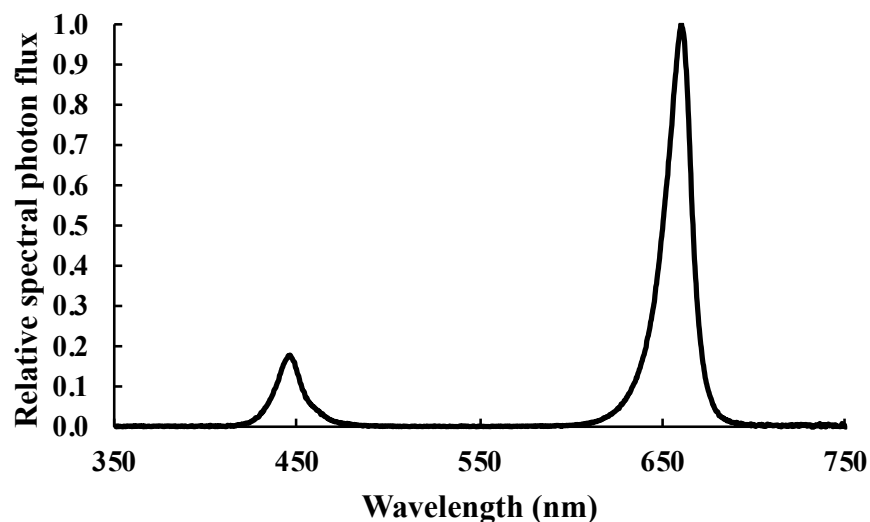
71
72 The optimum post-vegetative stage morphology varies depending on the cultivators' production
73 system (e.g., length of vegetative stage, plant density in both vegetative and flowering stages,
74 growing media type and rootzone volume, type of trellising system used in flowering, etc.), but
75 the general goal is to ensure high transplant success and strong vegetative growth (Vanhove et
76 al., 2011). The LI during the vegetative stage can influence plant growth attributes such as
77 height, stem thickness, branching, leaf size, leaf thickness, and biomass partitioning (Poorter et
78 al., 2019). Since these attributes affect a crop's robustness as it enters the flowering stage, the
79 vegetative stage LI must be selected to promote the development of the foundational structure
80 (e.g., thicker stems and more nodes) needed to support prolific inflorescence development, which
81 can account for more than half of the total aboveground biomass at peak maturity (Rodriguez-
82 Morrison et al., 2021).

83
84 The current lack of scientific information related to LI during the vegetative stage has resulted in
85 a broad range of canopy-level PPFDs (e.g., 250 to 650 $\mu\text{mol}\cdot\text{m}^{-2}\cdot\text{s}^{-1}$) being recommended to
86 cultivators (Fluence, 2020; Lumigrow, 2017). Since cannabis can tolerate (Chandra et al., 2008)
87 and even flourish (Rodriguez-Morrison et al., 2021) under very high LI, there is opportunity to
88 elevate PPFD during the vegetative stage to enhance plant structure and shorten the length of the
89 vegetative stage. Therefore, the objective of this study was to determine the effects of a broad
90 range of LI on vegetative stage cannabis morphology and growth attributes, to guide cultivators
91 towards optimizing the LI for their specific production strategies.

92

93 **Materials and Methods**

94 *Plant propagation and cultivation.* Uniform clonal cuttings of the cannabis genotype ‘Gelato-29’
 95 (short and bushy growth habit) were coated with 0.1% indole-3-butyric acid rooting hormone
 96 (StimRoot #1; Master Plant-Prod Inc., Brampton, ON, Canada) at the base of each cutting and
 97 inserted into cylindrical rockwool plugs (3.6 cm diameter × 4.0 cm height; Grodan, Milton, ON,
 98 Canada) at one cutting per plug. Plugs were pre-soaked in a preventative biological fungicide
 99 solution (RootShield WP; Bioworks, Victor, NY, USA) at 0.45 g·L⁻¹ in distilled water, with a
 100 final electrical conductivity (EC) of 0.7 dS·m⁻¹ and pH of 5.2. The plugs were placed in
 101 propagation trays (0.5 × 0.3 m, 50 Plug Pre-filled; A.M.A Horticulture Inc., Kingsville, ON,
 102 Canada) and covered with transparent plastic lids (0.29 × 0.55 × 0.19 m, 7-inch Propagation
 103 Dome; Mondi Products, Vancouver, BC, Canada). Cuttings were rooted for 14 d under a 16-h
 104 photoperiod with a targeted canopy-level PPFD of 200 μmol·m⁻²·s⁻¹ from light-emitting diodes
 105 (LEDs) (Toplight-Targeted Spectrum; Lumigrow, Emeryville, CA, USA). Only the blue (B, 400-
 106 500 nm) and red (R, 600-700 nm) channels were used, with peak wavelengths and full-width at
 107 half maximum (FWHM) of 445 nm and 17 nm for red and 665 nm and 16 nm for blue, and a
 108 photon flux ratio of B15:R85 (Fig. 1). Spectrum and LI were evaluated using a radiometrically-
 109 calibrated spectrometer (XR-Flame-S; Ocean Optics, Dunedin, FL, USA) coupled to a CC3
 110 cosine-corrector attached to a 1.9 m × 400 μm UV-Vis optical fibre. The intensities of B and R
 111 LEDs were modified using the lighting control software (smartPAR; Lumigrow) to achieve the
 112 prescribed PPFD and B:R.



113
 114 Figure 1. Relative spectral photon flux distribution of blue (B) and red (R) LEDs used during the
 115 propagation and vegetative stages.

116
 117 Uniformly-sized rooted cuttings with height and number of nodes of (mean ± SE, n = 90) 13 ±
 118 0.2 cm and 5 ± 0.1, respectively, were transplanted into rockwool blocks (0.15 × 0.15 × 0.15 m,
 119 Grodan) and grown for 21 d under a 16-h photoperiod. The initial height, measured from
 120 substrate surface to the highest point on the plant, and the number of nodes for each plant were
 121 recorded. The transplants were not irrigated for the first three days to encourage root growth and
 122 were then drip-irrigated twice daily at 2 L·hr⁻¹ for 540 s, such that each plant received roughly
 123 0.6 L·d⁻¹. The nutrient solution was comprised of Dutch Nutrients Gro A and Gro B

124 (Homegrown Hydroponics, Toronto, ON, Canada) at a rate of $5 \text{ mL}\cdot\text{L}^{-1}$ in rain water, resulting in
125 an EC of $\approx 1.8 \text{ dS}\cdot\text{m}^{-1}$ and pH of ≈ 5.7 .

126
127 The experiment was conducted in a commercial cannabis greenhouse facility in Southern
128 Ontario, Canada. Three enclosures ($5.9 \times 4.1 \times 2.7 \text{ m}$) were used, each consisting of two benches
129 ($5.9 \times 1.8 \text{ m}$) that were separated by 0.5 m and encompassed with panda film (Vivosun, City of
130 Industry, CA, USA) – black side facing inwards – to block natural light and minimize solar
131 heating. Each enclosure was divided into five $\times 1 \text{ m}^2$ plots, with a minimum lateral separation of
132 0.65 m between the edges of adjacent plots. Each plot consisted of 12 plants (i.e., 12 plants/ m^2),
133 arranged in four rows of three plants each, such that all plants were equally spaced. The plants in
134 the outer rows were border plants while the six plants in the inner rows were measured
135 experimentally (i.e., treatment plants). Plants were irrigated using the same nutrient solution that
136 was used during the transplant stage (described above). Air temperature and relative humidity
137 (RH) were recorded every 300 s using data loggers (HOBO MX2301A; Onset Computer
138 Corporation, Bourne, MA, USA) located at light fixture level in each enclosure. Across the three
139 enclosures, the daytime temperature and RH were (mean \pm SD, $n = 3$) $25 \pm 0.3 \text{ }^\circ\text{C}$ and $37 \pm 0.6\%$
140 [i.e., vapor pressure deficit (VPD) $\approx 2.0 \text{ kPa}$], respectively, and nighttime temperature and RH
141 were $22 \pm 0.1 \text{ }^\circ\text{C}$ and $40 \pm 0.6\%$ (i.e., VPD $\approx 1.6 \text{ kPa}$), respectively.

142
143 *Light intensity treatments.* This experiment was arranged as a randomized complete block design
144 (RCBD) with five target LI treatments (200, 450, 700, 950, and $1200 \mu\text{mol}\cdot\text{m}^{-2}\cdot\text{s}^{-1}$) using the
145 same light fixtures and spectrum from the propagation stage (described above) and three
146 concurrent replications (i.e., the enclosures). Pairs of LED bars ($1.09 \times 0.11 \text{ m}$) were spaced 0.4
147 m apart ‘on-center’ over each plot. For the $1200 \mu\text{mol}\cdot\text{m}^{-2}\cdot\text{s}^{-1}$ treatment plots, an additional pair
148 of LED bars were evenly spaced between the first pair of LED bars. All treatments had a
149 photoperiod of 16 h (0600 HR to 2200 HR). Spectrum and PPFD, at initial canopy level, were set
150 (as described above) using smartPAR (Lumigrow) and the spectrometer (Ocean Optics).
151 Following initial setup, the PPFD at the top of each plant was measured and recorded twice
152 weekly using a quantum sensor (LI-180; LI-COR Biosciences, Lincoln, NE, USA), and the
153 fixture hang-heights were adjusted accordingly, to maintain consistent canopy-level PPFDs
154 throughout the trial.

155
156 Although the layout of the experiment was a RCBD, the trial was conducted as a gradient design
157 (Jones-Baumgardt et al., 2020; Rodriguez-Morrison et al., 2021) with each plant treated as an
158 experimental unit and assigned a LI level consistent with their respective accumulated light
159 histories. To this end, the average PPFD (APPFD) each individual plant received over the trial
160 was obtained by computing the light integrals between each bi-weekly PPFD measurement
161 period, summing these integrals over the entire trial to determine a total light integral (TLI,
162 $\text{mol}\cdot\text{m}^{-2}$), and then back-calculating to determine APPFD by dividing TLI by the total number of
163 seconds of lighting during the trial (i.e., $3600 \text{ s}\cdot\text{hr}^{-1} \times 16 \text{ hr}\cdot\text{d}^{-1} \times 21 \text{ d}$).

164
165 *Plant growth and leaf morphology.* The plants were harvested 21 d after the start of the LI
166 treatments. Final height and number of nodes for each plant were recorded. Increases in height
167 (ΔH) and number of nodes (ΔNN) were determined by subtracting initial values from harvest
168 values. Internode length (IL) was determined by dividing ΔH by ΔNN . The width of each plant
169 was measured as the maximum lateral spread in two perpendicular axes based on the geographic

170 orientation on the bench: north-south (N-S) and east-west (E-W). Growth index (GI) was
171 calculated using the following equation: $[(\text{Final height} \times \text{Width}_{\text{N-S}} \times \text{Width}_{\text{E-W}}) / 300]$ (from
172 Ruter, 1992). Chlorophyll content index (i.e., SPAD) was measured three times (then averaged)
173 on one of the youngest fully-expanded leaves using a chlorophyll meter (SPAD 502; Spectrum
174 Technologies Inc., Aurora, IL, USA). Stem thickness (ST) was measured at the first internode
175 using a digital caliper. The stem of each plant was cut at substrate level and aboveground fresh
176 weight (FW) was measured using a digital scale (AX622N/E Adventure Precision Balance;
177 OHAUS Corporation, Parsippany, NJ, USA). All aboveground tissues were dried to constant
178 weight at 65 °C and re-weighed to determine dry weight (DW). Aboveground tissue water
179 content (WC) was calculated using the following equation: $[(\text{FW} - \text{DW}) / \text{FW}] \times 100\%$. Single
180 leaves from the tenth node from the bottom of each plant were scanned (CanoScan LiDE 25;
181 Canon Inc., Japan) at 600 dpi resolution and then dried to constant weight at 65 °C. Leaf size
182 (cm^2/leaf) was computed from the digital images using ImageJ (Version 1.52q; National
183 Institutes of Health, Bethesda, MD, USA). The DW of each scanned leaf was determined using
184 an analytical balance (AE 100; Mettler Toledo, Columbus, OH, USA) and specific leaf weight
185 (SLW; $\text{mg}\cdot\text{cm}^{-2}$) was determined by dividing leaf DW by leaf size.

186
187 *Data processing.* All data were analyzed using least-squares non-linear regression in Prism
188 (GraphPad Software, San Diego, CA, USA) with APPFD as the independent variable, to
189 determine the best-fit model for each attribute ($P \leq 0.05$). The models tested were linear,
190 quadratic, and asymptotic. Outliers were detected and removed using a Q-coefficient of 1.0 in
191 Prism's ROUT outlier detection algorithm. For quadratic responses, the vertices were calculated
192 to determine the light saturation points (LSP) for each attribute. The asymptotic equation: $Y = a$
193 $+ be^{(kX)}$, where Y, a, e, and X represent the measured attribute, maximum value for the measured
194 attribute (i.e., the horizontal asymptote), Euler's number, and APPFD, respectively, was used to
195 model non-linear relationships that did not have a vertex within the tested APPFD range. For
196 asymptotic models, maximum quantum efficiency (MQE) was derived from the slope of the
197 linear portion of the models, over the APPFD range of 130 to 200 $\mu\text{mol}\cdot\text{m}^{-2}\cdot\text{s}^{-1}$. Further, PPFD₂₀
198 (i.e., a practical LSP) was defined for the asymptotic models as the APPFD level where the
199 localized slope of the curve fell below 20% of the slope at MQE. The PPFD₂₀ was used to
200 indicate that increasing the APPFD beyond this level resulted in minimal further increases in the
201 respective responses; thus, acting as a proxy for a LI-response efficiency threshold.

202 203 **Results**

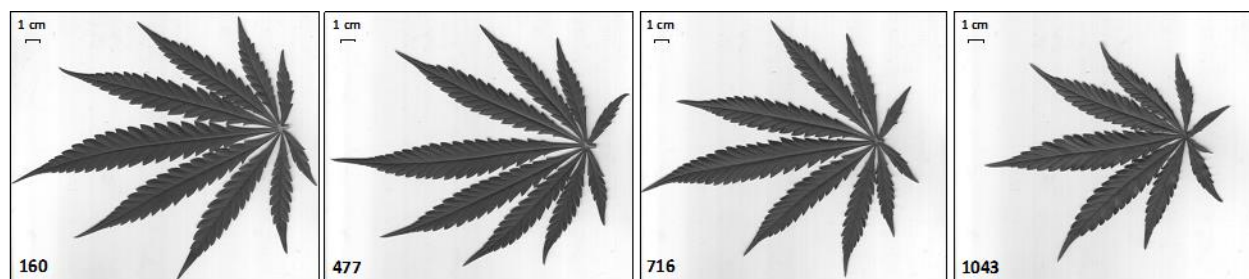
204 The range of APPFDs that plants grew under in this trial was 135 to 1430 $\mu\text{mol}\cdot\text{m}^{-2}\cdot\text{s}^{-1}$,
205 corresponding to daily light integrals (DLI) ranging from 7.8 to 82 $\text{mol}\cdot\text{m}^{-2}\cdot\text{d}^{-1}$. Notably, there
206 were no signs of transplant shock or light stress, even in plants placed under the highest LIs
207 (which were up to 7 times higher than the LI in the propagation stage). Overall, plants grown
208 under different LIs exhibited varying architectures (Fig. 2) and leaf morphology (Fig. 3).
209 Generally, plants grown under high LI had more compact, denser growth, resulting in shorter
210 plants, greater numbers of potential flowering sites, and higher aboveground biomass. However,
211 individual measured growth attributes had varying responses to increasing LI. While some
212 attributes exhibited linear responses to LI, several attributes exhibited saturating responses to
213 increasing LI, and others had maxima at moderate APPFD levels.

214

215

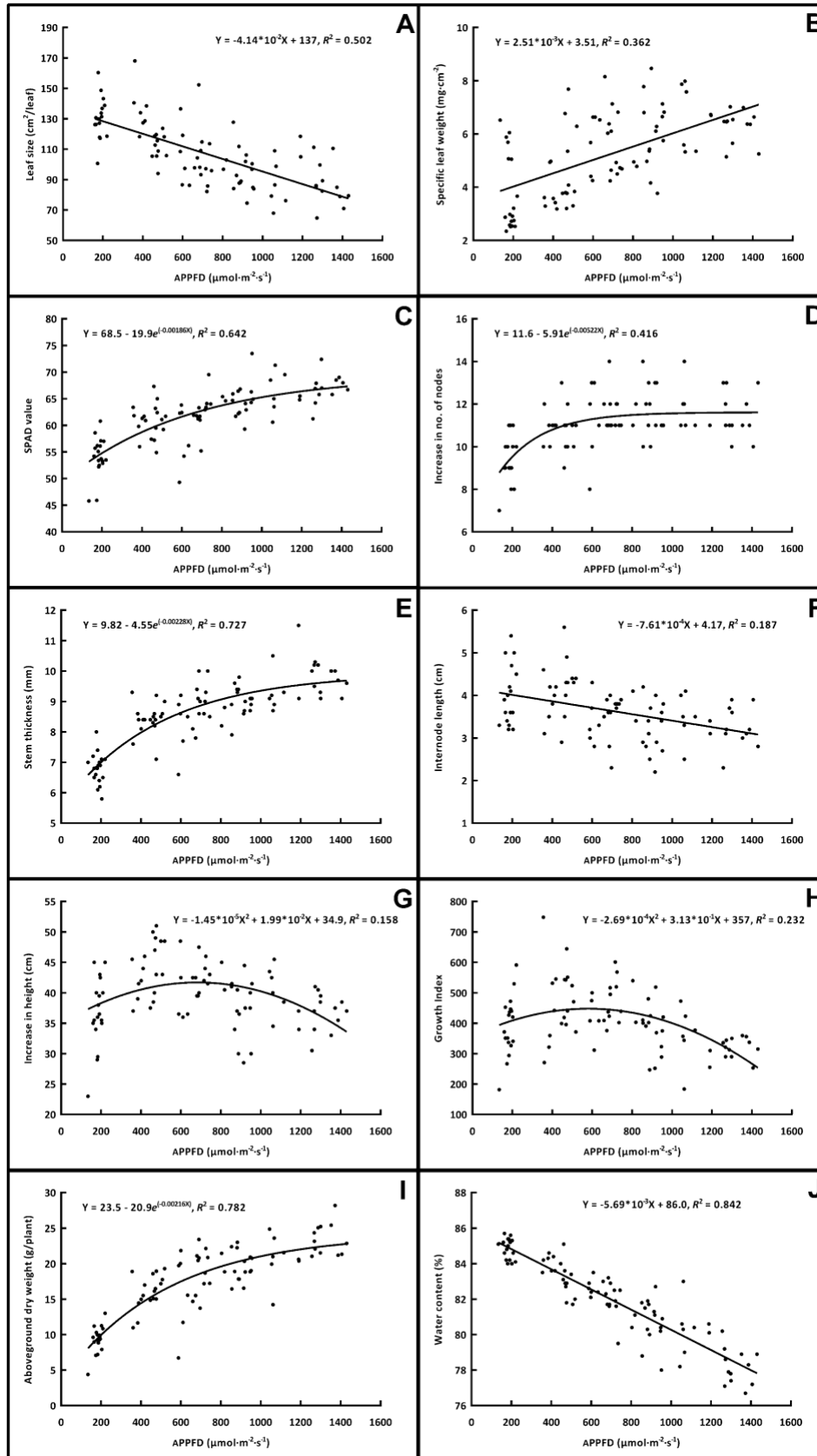


216 Figure 2. Cannabis plants after growing under canopy-level average photosynthetic photon flux
 217 densities (APPFD) of 179, 478, 713, 917, and 1367 $\mu\text{mol}\cdot\text{m}^{-2}\cdot\text{s}^{-1}$ with a 16-h photoperiod for 21
 218 d.
 219



220 Figure 3. Single cannabis leaves taken at the tenth node after growing under canopy-level
 221 average photosynthetic photon flux densities (APPFD) of 160, 477, 716, and 1043 $\mu\text{mol}\cdot\text{m}^{-2}\cdot\text{s}^{-1}$
 222 with a 16-h photoperiod for 21 d.
 223

224 Increasing LI resulted in smaller leaflets with smaller, more numerous serrations along the leaflet
 225 margins (Fig. 3). Individual leaf size decreased linearly (Fig. 4A) and individual leaf biomass
 226 increased linearly (data not shown) resulting in an 84% increase in SLW (Fig. 4B) at the
 227 maximum vs. minimum APPFD. SPAD, an area-based index of chlorophyll content, increased
 228 asymptotically with increasing LI, and was 24% higher at the PPF_{D20} of 1030 vs. 135 $\mu\text{mol}\cdot\text{m}^{-2}\cdot\text{s}^{-1}$
 229 $\mu\text{mol}\cdot\text{m}^{-2}\cdot\text{s}^{-1}$ (Fig. 4C). The ΔNN and ST also increased asymptotically with increasing LI, with
 230 respective PPF_{D20} of 472 and 870 $\mu\text{mol}\cdot\text{m}^{-2}\cdot\text{s}^{-1}$, where ΔNN and ST were 28% and 41% higher
 231 vs. the minimum APPFD (Fig. 4D and E). The IL decreased linearly with increasing LI, resulting
 232 in 24% shorter internodes at the maximum vs. minimum APPFD (Fig. 4F). Both ΔH and GI (of
 233 which final height is a coefficient) had quadratic responses to LI, with maxima at 686 and 582
 234 $\mu\text{mol}\cdot\text{m}^{-2}\cdot\text{s}^{-1}$, respectively (Fig. 4G and H). The maximum ΔH was 12% and 24% higher than at
 235 the minimum and maximum APPFD, respectively and the maximum GI was 14% and 76%
 236 higher than at the minimum and maximum APPFD, respectively. Aboveground DW increased
 237 asymptotically with increasing LI and was 2.6 times higher at the PPF_{D20} of 910 vs. the
 238 minimum APPFD (Fig. 4I) while WC decreased linearly by 9% at maximum vs. minimum
 239 APPFD (Fig. 4J).



241 Figure 4. Individual leaf area (A) and specific leaf weight of individual leaves taken at the tenth
242 node (B), leaf chlorophyll content index (i.e., SPAD value) of the youngest fully-expanded leaf
243 (C), increase in the number of nodes (D), stem thickness (E), internode length (F), increase in
244 height (G), growth index (H), aboveground dry weight (I), and aboveground plant tissue water
245 content (J) of vegetative cannabis plants grown for 21 d under average photosynthetic photon
246 flux densities (APPFD) ranging from 135 to 1430 $\mu\text{mol}\cdot\text{m}^{-2}\cdot\text{s}^{-1}$. Each data point represents an
247 individual plant with its own APPFD.

248

249 Discussion

250 In the indoor cannabis production industry, there is considerable variability in the
251 characterization of what constitutes an optimum structure of clonal plants prior to the initiation
252 of the (flower-inducing) short-day photoperiod. This is due to myriad factors, including:
253 genotypic specific growth habit [e.g., indica- vs. sativa-dominant plant structure (Jin et al.,
254 2021)], size of plants, substrate volume, cropping density, environmental settings (including LI),
255 and many cultivator-specific plant husbandry practices such as periodic de-leafing and utilization
256 of plant training (e.g., stakes, trellis-supports, etc.). Notwithstanding these variances, the
257 underlying goals of the vegetative stage are steadfast: to produce healthy, resilient plants that are
258 capable of supporting prolific inflorescence biomass production, from both assimilative and
259 structural perspectives. Therefore, within the aforementioned cultivator-specific constraints,
260 plants coming out of the vegetative stage should have a general structure that is primed to
261 optimize future photosynthetic capacity, facilitate airflow within the crop canopy, maximize
262 potential flowering sites, and bear the weight of the mature inflorescences. These parameters
263 necessitate plants that have foliar architecture and morphology capable of intercepting and
264 utilizing the incoming *PAR*, with as many nodes as possible [cannabis flower buds arise from
265 foliar axils (Spitzer-Rimon et al., 2019)], and that have relatively compact growth (i.e., short
266 internodes) with robust stems.

267

268 Key plant morphological and physiological attributes have shown varying responses to LI. In a
269 comprehensive review paper, Poorter et al. (2019) summarized the characteristic responses of
270 many attributes from myriad herbaceous and woody plants using relative response models over
271 DLIs up to 50 $\text{mol}\cdot\text{m}^{-2}\cdot\text{d}^{-1}$ (i.e., equivalent to $\approx 870 \mu\text{mol}\cdot\text{m}^{-2}\cdot\text{s}^{-1}$ in the present study).
272 Extrapolating their findings to the APPFD range in the present study, they found that individual
273 leaf area decreased by $\approx 23\%$ and SLW nearly doubled with increasing LI, although there were
274 no LI treatment effects on area-based chlorophyll content. The LI treatment effects on leaf
275 morphology were somewhat smaller in Poorter et al. (2019) compared to the present study,
276 suggesting that cannabis may have relatively high phenotypic plasticity for leaf morphology
277 adaptations to LI. However, the present study observed a 24% increase in area-based chlorophyll
278 content, which may indicate that cannabis favours upregulating photosynthetic capacity (i.e.,
279 maximizing resource utilization) over the common foliar morphology-based adaptive responses
280 to high light stress. **Clonal cannabis' very high photosynthetic capacity (Chandra et al., 2008;
281 Rodriguez-Morrison et al., 2021) appears to be present even at the relatively young vegetative
282 stage (Chandra et al., 2015). In the context of indoor production, the reduction in individual leaf
283 area with increasing LI may also confer an increase in whole-plant net photosynthesis, since a
284 greater proportion of the incident *PAR* should penetrate deeper into the canopy through inherent
285 reductions in self-shading. Moreover, leaves with higher SLW, which is strongly correlated with
286 leaf thickness (Vile et al., 2005; Wilson et al., 1999), can increase water use efficiency (Yun and**

287 Taylor, 1986), enhance resistance to pathogens (Guest and Brown, 1997), and minimize
288 mechanical damage.

289
290 The intensity of *PAR* in the vegetative stage can have major influences on plant structure during
291 this short but critical stage of production. Though not often reported (because it is a destructive
292 measurement), aboveground biomass (i.e., DW) is perhaps the single most comprehensive
293 parameter that relates LI effects on vegetative growth. As it does in floral and non-floral biomass
294 at optimum inflorescence maturity (Rodriguez-Morrison et al., 2021), DW during the vegetative
295 stage had a strong linear response to increasing LI. There was almost a 3-fold increase in DW
296 over the 135 to 1430 $\mu\text{mol}\cdot\text{m}^{-2}\cdot\text{s}^{-1}$ Δ PPFD range in the present study, although 90% of the
297 maximum increase in DW was attained at an APPFD of only $\approx 900 \mu\text{mol}\cdot\text{m}^{-2}\cdot\text{s}^{-1}$. Further,
298 aboveground tissue moisture content decreased linearly with increasing LI (Fig. 4J), which is a
299 common response to LI (Poorter et al., 2019) that normally confers an increase in mechanical
300 strength (Shah et al., 2017). Both Δ H and GI were maximized at moderate APPFD levels of \approx
301 $600 \mu\text{mol}\cdot\text{m}^{-2}\cdot\text{s}^{-1}$. While these are generally negative characteristics in the context of vegetative-
302 stage cannabis, open plant architectures may benefit denser genotypes (e.g., indica-dominant) by
303 increasing the airflow within the canopy, potentially suppressing foliar pests while making
304 routine pest monitoring easier (Bakro et al., 2018; Chandra et al., 2017). In contrast, plants were
305 smaller at ≈ 900 vs. $600 \mu\text{mol}\cdot\text{m}^{-2}\cdot\text{s}^{-1}$ but had $\approx 15\%$ higher DW and $\approx 6\%$ thicker stems (i.e., \approx
306 13% higher cross-sectional area). Since the number of nodes saturated at relatively low LI, a
307 canopy-level PPF target of about $900 \mu\text{mol}\cdot\text{m}^{-2}\cdot\text{s}^{-1}$ may be most appropriate for producing
308 robust but not overly compact plants while also minimizing lighting-related energy and
309 infrastructure costs. Although not as common in commercial settings, production facilities that
310 target more open plant architecture and greater energy conservation may opt for canopy-level
311 PPF target of $\approx 600 \mu\text{mol}\cdot\text{m}^{-2}\cdot\text{s}^{-1}$.

312
313 Another consideration is the adaptive capacity of vegetative plants to the normal increases in
314 canopy-level LI as they transition into the flowering phase, which are necessary to maintain the
315 DLI in conjunction with shortening the photoperiod to induce strong flowering responses –
316 normally from ≥ 16 h to ≤ 12 h (Potter, 2014). Therefore, to maintain the same DLI as in the
317 vegetative phase, the PPF must be increased by at least 25%. However, cannabis takes time to
318 acclimate its photosynthetic capacity to higher LIs when transitioning out of the vegetative phase
319 (Rodriguez-Morrison et al., 2021). Given vegetative cannabis' demonstrated capacity to
320 proliferate under high LIs, using canopy-level PPFs $\geq 900 \mu\text{mol}\cdot\text{m}^{-2}\cdot\text{s}^{-1}$, particularly in the
321 latter stages of the vegetative phase (i.e., after plants have recovered from transplant shock), may
322 optimize their adaptation to the higher LIs in the flowering phase while also potentially
323 shortening the vegetative phase.

324
325 The industry recommendations for LI during cannabis' vegetative stage are variable (e.g.,
326 Fluence, 2020; Lumigrow, 2017); however, few contemporary recommendations suggest
327 exposing vegetative cannabis plants to PPFs higher than $800 \mu\text{mol}\cdot\text{m}^{-2}\cdot\text{s}^{-1}$ in indoor production
328 systems. The current study demonstrates that vegetative cannabis can be exposed to substantially
329 higher LIs (than commonly-used in the industry) with positive morphological outcomes that can
330 prime plants for the transition into the flowering phase.

331

332

333 **Conclusion**

334 Within the parameters of this investigation, we observed that PPFD levels between 600 and 900
335 $\mu\text{mol}\cdot\text{m}^{-2}\cdot\text{s}^{-1}$ appeared to achieve an appropriate balance in optimizing key morphological
336 parameters in vegetative cannabis while minimizing energy use associated with excessively-high
337 LIs and also considering different production strategies. Although the desired morphological and
338 growth attributes of vegetative-stage clonal cannabis plants will be subjective to each genotype
339 and production scenario, the presented LI responses can assist cultivators in optimizing the LI for
340 their individual production goals; balancing the potential economic returns against elevated input
341 costs associated with supplying more PAR to their crops.

342

343 **Literature cited**

344 Arnold, J. M. 2013. Energy consumption and environmental impacts associated with *Cannabis*
345 cultivation. Humboldt State Univ., Arcata, MSc. Diss.

346

347 Bakro, F., W. Katarzyna, M. Bunalski, and M. Jedryczka. 2018. An overview of pathogen and
348 insect threats to fibre and oilseed hemp (*Cannabis sativa* L.) and methods for their biocontrol.
349 Integrated Control in Oilseed Crops 136:9–20.

350

351 Benke, K. and B. Tomkins. 2017. Future food-production systems: vertical farming and
352 controlled-environment agriculture. Sustainability: Sci. Practice Policy 13(1):13–26.

353 <https://doi.org/10.1080/15487733.2017.1394054>

354

355 Bilodeau, S.E., B. Wu, A. Rufyikiri, S. MacPherson, and M. Lefsrud. 2019. An update on plant
356 photobiology and implications for cannabis production. Frontiers Plant Sci. 10:296.

357 <https://doi.org/10.3389/fpls.2019.00296>

358

359 Caplan, D., J. Stemeroff, M. Dixon, and Y. Zheng. 2018. Vegetative propagation of cannabis by
360 stem cuttings: effects of leaf number, cutting position, rooting hormone and removal of leaf tips.

361 Can. J. Plant Sci. 98(5): 1126–1132. <https://doi.org/10.1139/cjps-2018-0038>

362

363 Carpentier, C., K. Mulligan, L. Laniel, D. Potter, B. Hughes, L. Vandam, D. Olszewski, and K.
364 Skarupova. 2012. Botany and cultivation of cannabis, p. 20–39. In: C. Carpentier, L. Laniel, and

365 P. Griffiths (eds.). Cannabis production and markets in Europe. European Monitoring Centre for
366 Drugs and Drug Addiction, Lisbon, Portugal. <https://doi.org/10.2810/76378>

367

368 Chandra, S., H. Lata, I.A. Khan, and M.A. Elsohly. 2008. Photosynthetic response of *Cannabis*
369 *sativa* L. to variations in photosynthetic photon flux densities, temperature and

370 CO₂ conditions. Physiol. Mol. Biol. Plants 14(4):299–306. [https://doi.org/10.1007/s12298-008-](https://doi.org/10.1007/s12298-008-0027-x)

371 [0027-x](https://doi.org/10.1007/s12298-008-0027-x)

372

373 Chandra, S., H. Lata, I.A. Khan, and M.A. ElSohly. 2017. *Cannabis sativa* L.: botany and
374 horticulture, p. 79–100. In: S. Chandra, H. Lata, and M.A. ElSohly (eds.). *Cannabis sativa* L. –

375 botany and biotechnology. Springer Nature, Cham, Switzerland. [https://doi.org/10.1007/978-3-](https://doi.org/10.1007/978-3-319-54564-6)

376 [319-54564-6](https://doi.org/10.1007/978-3-319-54564-6)

377

- 378 Chandra, S., H. Lata, and M.A. ElSohly. 2020. Propagation of cannabis for clinical research: An
379 approach towards a modern herbal medicinal products development. *Frontiers Plant Sci.* 11:958.
380 <https://doi.org/10.3389/fpls.2020.00958>
- 381
382 Chandra, S., H. Lata, Z. Mehmedic, I.A. Khan, and M.A. ElSohly. 2015. Light dependence of
383 photosynthesis and water vapor exchange characteristics in different high Δ^9 -THC yielding
384 varieties of *Cannabis sativa* L. *J. Appl. Res. Medicinal Aromatic Plants* 2(2):39-47.
385 <https://doi.org/10.1016/j.jarmap.2015.03.002>
- 386
387 Despommier, D. 2013. Farming up the city: The rise of urban vertical farms. *Trends Biotechnol.*
388 31:388–389. <https://doi.org/10.1016/j.tibtech.2013.03.008>
- 389
390 Fluence. 2020. Cannabis cultivation guide. Fluence, Austin, TX.
- 391
392 Guest, D. and J. Brown. 1997. Plant defences against pathogens, p. 263–286. In: J.F. Brown and
393 H.J. Ogle (eds.). *Plant pathogens and plant diseases*. Rockvale Publications, Armidale, Australia.
- 394
395 Jin, D., P. Henry, J. Shan, and J. Chen. 2021. Identification of phenotypic characteristics in three
396 chemotype categories in the genus *Cannabis*. *HortScience* 1-10.
397 <https://doi.org/10.21273/HORTSCI15607-20>
- 398
399 Jones-Baumgardt, C., D. Llewellyn, and Y. Zheng. 2020. Different microgreen genotypes have
400 unique growth and yield responses to intensity of supplemental PAR from light-emitting diodes
401 during winter greenhouse production in Southern Ontario, Canada. *HortScience* 55(2):156-163.
402 <https://doi.org/10.21273/HORTSCI14478-19>
- 403
404 Lumigrow. 2017. LED grower's guide for cannabis. Lumigrow, Emeryville, CA.
- 405
406 Mehboob, N., H.E.Z. Farag, and A.M. Sawas. 2020. Energy consumption model for indoor
407 cannabis cultivation facility. *J. Power Energy* 7:222–233. <https://doi.org/10.1109/OAJPE.2020.3003540>
- 408
409 Mills, E. 2012. The carbon footprint of indoor Cannabis production. *Energy Policy* 46:58–67.
410 <https://doi.org/10.1016/j.enpol.2012.03.023>
- 411
412 Poorter, H., Ü. Niinemets, N. Ntagkas, A. Siebenkäs, M. Mäenpää, S. Matsubara, and T.L. Pons.
413 2019. A meta-analysis of plant responses to light intensity for 70 traits ranging from molecules to
414 whole plant performance. *New Phytologist* 223:1073–1105. <https://doi.org/10.1111/nph.15754>
- 415
416 Potter, D.J. 2014. A review of the cultivation and processing of cannabis (*Cannabis sativa* L.) for
417 production of prescription medicines in the UK. *Drug Testing Analysis* 6(1–2):31–38.
418 <https://doi.org/10.1002/dta.1531>
- 419
420 Rodriguez-Morrison, V., D. Llewellyn, and Y. Zheng. 2021. Cannabis yield, potency, and leaf
421 photosynthesis respond differently to increasing light levels in an indoor environment. *Preprints*.
422 <https://doi.org/10.20944/preprints202101.0163.v1> and
423 <https://www.frontiersin.org/articles/10.3389/fpls.2021.646020/abstract>
- 424

- 425 Ruter, J.M. 1992. Influence of source, rate, and method of applying controlled release fertilizer
426 on nutrient release and growth of ‘Savannah’ holly. *Fertilizer Res.* 32(1):101–106.
427 <https://doi.org/10.1007/BF01054399>
428
- 429 Shah, D.U., T.P. Reynolds, and M.H. Ramage. 2017. The strength of plants: theory and
430 experimental methods to measure the mechanical properties of stems. *J. Expt. Bot.* 68(16):4497-
431 4516. <https://doi.org/10.1093/jxb/erx245>
432
- 433 Spitzer-Rimon, B., S. Duchin, N. Bernstein, and R. Kamenetsky. 2019. Architecture and
434 florogenesis in female *Cannabis sativa* plants. *Frontiers Plant Sci.* 10:350.
435 <https://doi.org/10.3389/fpls.2019.00350>
436
- 437 Vanhove, W., P. Van Damme, and N. Meert. 2011. Factors determining yield and quality of
438 illicit indoor cannabis (*Cannabis* spp.) production. *Forensic Sci. Intl.* 212(1–3):158–163.
439 <https://doi.org/10.1016/j.forsciint.2011.06.006>
440
- 441 Vile, D., E. Garnier, B. Shipley, G. Laurent, M.L. Navas, C. Roumet, S. Lavorel, S. Díaz, J.G.
442 Hodgson, F. Lloret, G.F. Midgley, H. Poorter, M.C. Rutherford, P.J. Wilson, and I.J. Wright.
443 2005. Specific leaf area and dry matter content estimate thickness in laminar leaves. *Ann.*
444 *Bot.* 96(6):1129-1136. <https://doi.org/10.1093/aob/mci264>
445
- 446 Wilson, P.J., K.E.N. Thompson, and J.G. Hodgson. 1999. Specific leaf area and leaf dry matter
447 content as alternative predictors of plant strategies. *New Phytologist* 143(1):155-162.
448 <https://doi.org/10.1046/j.1469-8137.1999.00427.x>
449
- 450 Yun, J.I. and S.E. Taylor. 1986. adaptive implications of leaf thickness for sun-and shade-grown
451 *Abutilon theophrasti*. *Ecology* 67(5):1314–1318. <https://doi.org/10.2307/1938687>